Temperature measurement of a heated surface with a honeycomb porous plate in burnout occurrence in a saturated pool boiling of a nanofluid

SHOJI MORI and RYUTA YANAGISAWA
Department of Chemical Engineering Science
Yokohama National University
79-5, Tokiwadai, Hodogaya-ku, Yokohama
JAPAN
morisho@ynu.ac.jp

Abstract: - A honeycomb-structured ceramic porous plate (HPP) was used to increase the critical heat flux (CHF) in a saturated pool boiling. The HPP employed was a commercially available filter normally used to purify exhaust gases from combustion engines. Combining the HPP with a nanofluid significantly improved the CHF compared to that obtained from a plain surface in pure water, to a maximum of approximately 3.2 MW/m^2. In this paper, the mechanism for the CHF enhancement was considered by measuring the temperature of the heated surface using an ITO heater and a high-speed infrared camera. As a result, the following conclusions can be made based on the out data. The average temperatures at the intersecting parts of the HPP were relatively high (more than 200 °C) compared to other locations. And when the HPP was installed on the heated surface in conjunction with the nanofluid, the wall temperatures obtained under burnout conditions decreased in the order of the intersection of an HPP wall > an HPP wall between intersections > the cell. However, dryout was initiated in the cell and a wall temperature of 330 °C was first obtained in this location when burnout occurred. This result implies that further CHF improvements could be achieved if the initiation of dryout at the cell can be suppressed.

Key-Words: boiling, CHF enhancement, IR camera, honeycomb porous plate

1 Introduction

One strategy for dealing with serious incidents is the in-vessel retention (IVR) of corium debris. IVR consists of external cooling of the reactor vessel in order to remove decay heat from the molten core through the lower head of the vessel. However, the extent of heat removal is limited by the critical heat flux (CHF) at the outer surface of the vessel. Therefore, in order to enhance the IVR, it is important to devise methods of increasing the CHF. Approaches to increasing the IVR capacity must be both simple and installable at low cost, while associated cooling techniques should be applicable to a large heated surface.

Our group has previously demonstrated enhancement of the CHF of a large heated surface using a porous plate with a honeycomb structure immersed in a saturated pool boiling system based on distilled water [1-3]. Experimental data confirmed that this method essentially doubled the CHF (to a value of approximately 2.0 MW/m^2) relative to that of a plain surface, when using a plate with a diameter of 30 mm [1]. Moreover, depositing nanoparticles on the surface of a 50 mm porous plate, to produce an essentially infinite surface area [4], increased the CHF by a factor of 2.2 times (to 2.2 MW/m^2) [3] as compared to a plain surface. This technique allows the rapid removal of heat simply via the attachment of the nanoparticle-deposited porous plate to the heated surface [3]. A honeycomb porous plate (HPP) has been combined with a nanofluid so as to obtain a synergistic effect. This combination greatly improves the CHF, giving a value of approximately 3.2 MW/m^2 in conjunction with a copper block heater [5]. However, the CHF enhancement mechanism by an HPP together with a nanofluid is not yet fully understood, because variations in the wall temperature distribution with time just below

the HPP cannot be observed when using a copper block heater. Therefore, in the present paper, changes in the temperature distribution on a heated surface over time up to the point of burnout were assessed using an indium tin oxide (ITO) heater and a high-speed infrared (IR) camera. The resulting data are used to examine the CHF enhancement mechanism obtained from combining an HPP with a nanofluid.

2 Experimental apparatus and procedure

2.1 Experimental apparatus

Fig. 1 shows the experimental setup in which an ITO heater is used in order to measure the temperature distribution of the heated surface with a high-speed IR camera. The main vessel, which is made of Pyrex glass, had an inner diameter of 87 mm and a height of 500 mm. The pool container was filled with distilled water or nanofluid to a height of approximately 60 mm above the heated surface.

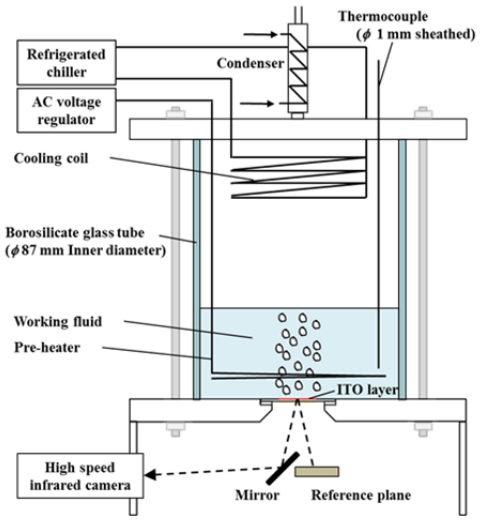

Fig. 1 Schematic diagram of the experimental apparatus including the pool boiling system and ITO heater.

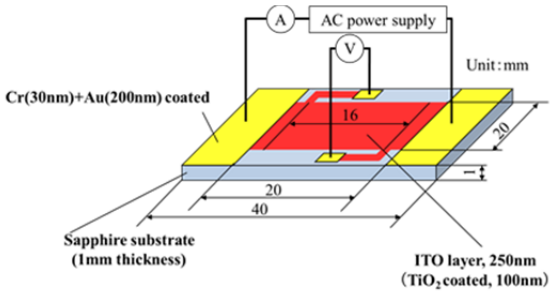

Fig. 2 ITO heater.

Fig. 2 depicts the ITO heater used in the present study. This device was fabricated by vacuum depositing a 250 nm thick ITO film on a sapphire substrate (1 × 40 × 40 mm). The heating area of the ITO unit was 20 × 20 mm. The heater was installed with the ITO film facing upward and, in order to improve wettability, the film was coated with a 100 nm thick layer of TiO_2 because ITO is hydrophobic. Cr (30 nm thick) and Au (200 nm thick) electrodes were deposited sequentially on the sapphire substrate, and were connected to an AC power supply to control the heat flux at the surface. The heating cycle frequency of the AC power supply had to be as high as possible so as not to affect primary bubble generation. Thus, in the present study, the heating frequency was set to 1000 Hz, based on a consideration of the frequency of primary bubble detachment.

The temperature distribution on the heated ITO surface was obtained using an IR high-speed camera with spatial and time resolutions of 130 μm and 2 ms, respectively. A similar technique has been previously demonstrated by Nakamura [6]. The use of a relatively thin ITO film (250 nm) meant that data acquired from the IR camera when viewing the underside of the film accurately reflected the temperature on the top of the heater surface.

2.2 Experimental procedure

Experiments were carried out using either distilled water or nanofluid as the working fluid under saturated conditions at atmospheric pressure. A sheathed heater was installed above the heated surface in the liquid bath in order to maintain the liquid temperature at the saturation

temperature. During each trial, the heat flux was increased in increments of approximately 0.1 MW/m^2 until the CHF condition was reached, defined as a rapid wall temperature increase. The final heat flux in the quasi-steady state was then measured before the transition to film boiling and was taken as equal to the CHF.

2.3 Honeycomb porous plates

Fig. 3 show the HPP used in the present study, including a micrograph of its structure on the right-hand side of the figure. This device, which is commercially available, is intended for use as a filter for purifying exhaust gases from combustion engines and is composed of $CaOAl_2O_3$ (30-50 wt%), fused SiO_2 (40-60 wt%) and TiO_2 (5-20 wt%). The vapor escape channel width (equivalent to the cell width), d_V, the wall thickness of the grid, δ_S, the aperture ratio (the ratio of the open area to total area), the height, δ_h, and the diameter of the HPP were 1.3 mm, 0.4 mm, 0.55, 1.0 mm and 30.0 mm, respectively. The pore radius distribution of the HPP was determined by mercury penetration porosimetry and was found to peak at approximately 0.17 μm. The average pore radius, the median pore radius, and the porosity of the HPP as determined by porosimetry were 0.037 μm, 0.13 μm, and 24.8%, respectively. The HPP was held against the top of the heater using a stainless steel plate and a silicone rubber sheet. No thermally conductive grease was applied between the plate and either heated surface.

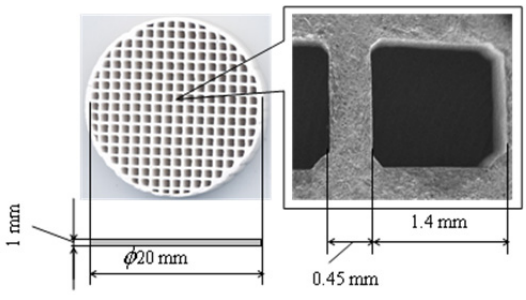

Fig. 3 Honeycomb porous plate.

2.4 Preparation of the nanofluid

Titanium oxide (TiO_2) nanoparticles purchased from the Aerosil Corporation (Aeroxide TiO_2 P 25) with a mean particle size of 21 nm were used in the present study. Water-based nanofluids were prepared by dispersing the dry oxide in distilled water using ultrasonic vibration for 2 h. Additives such as surfactants or dispersants were not used to stabilize the nanoparticle suspensions. The concentrations of the oxide in the nanofluid were 0 vol.% (0 g/L), 0.001 vol.% (0.04 g/L), and 0.1 vol.% (4.0 g/L).

3. Experimental results and discussion

As noted, an HPP and a nanofluid can be combined to enhance the CHF to a significant extent [5]. In order to clarify the CHF enhancement mechanism, temperature measurements were performed over time just below the HPP using the high-speed IR camera.

Fig. 4 provides plots of the boiling curves. These data were acquired using distilled water with a plain surface, nanofluid at 0.1 vol.% with a plain surface, the HPP with distilled water, and the HPP with nanofluid at 0.1 vol.%. The arrows in Fig. 4 indicate the different CHF conditions. The boiling curves demonstrate that, in the presence of the plain surface, the CHF values were higher when using the nanofluid. This enhancement is attributed to the increased surface wettability, surface roughness, and capillary wicking effect resulting from nanoparticle deposition on the heated surface, as has also been reported in previous studies. The CHF was also higher when using the HPP in both the distilled water and nanofluid. The beneficial effect of the HPP is attributed to the automatic liquid supply to the heated surface due to capillary action and the reduced resistance to vapor escape flow due to the separation of the liquid and vapor flows by the honeycomb porous structure [1, 2]. Moreover, it is interesting to observe that the highest CHF was obtained from the combination of the HPP with the nanofluid.

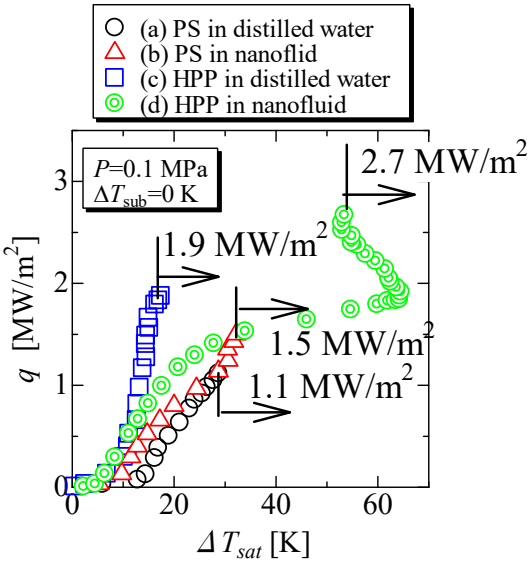

Fig. 4 Boiling curves and heat transfer coefficients obtained from trials using the ITO heater.

Fig. 5 indicates the changes in the IR images over time when using the HPP in the saturated pool boiling of the nanofluid (at 0.1 vol.%) under burnout conditions (2.84 MW/m^2), corresponding to the highest heat flux in all cases. As the high temperature region that corresponds to the dryout area repeatedly spreads and shrinks, the temperature of the central part of the heater sharply increases. Irreversible dry spots subsequently form and grow gradually, resulting in burnout. In the case of the HPP with the nanofluid, reversible dry spots can first be observed at a heat flux of 2.38 MW/m^2. Reversible dry spots were initiated in the cell part of the HPP, and small dry spots coalesced into a large irreversible dryout, leading to burnout. Frequent temperature increases occurred in the cell, although the wall temperature was reduced because the wall was easily wetted due to the nanoparticle deposition. The burnout always occurred when the wall temperature exceeded the Leidenfrost temperature, at which point the hovering period of coalesced bubbles was increased under the high heat flux and the dried area of the heating surface was not rewetted. When the HPP was installed on the heated surface in conjunction with the nanofluid, the average wall temperature under the burnout conditions decreased in the order of: the intersection of an HPP wall, an HPP wall between intersections, and the cell. However, the location where dryout first occurred and at which the wall temperature first reached 300 °C was always the cell of the HPP. This result suggests that the CHF may be further improved if the initiation of dryout at the cell can be suppressed.

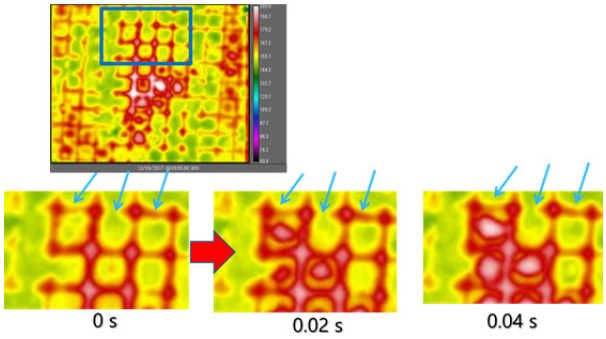

Fig. 5 Surface temperature change with time in burnout occurrence.(HPP + nanofluid , q=2.8 MW/m^2)

4. Conclusions

CHF enhancement resulting from a honeycomb-structured porous plate was investigated experimentally using a saturated pool boiling system in conjunction with a nanofluid. The following conclusions can be made based on the resulting data.

1. Temperature measurements by high-speed IR camera demonstrated that the average temperatures at the intersecting parts of the HPP were relatively high (more than 200 °C) compared to other locations.

2. When the HPP was installed on the heated surface in conjunction with the nanofluid, the wall temperatures obtained under burnout conditions decreased in the order of the intersection of an HPP wall > an HPP wall between intersections > the cell. However, dryout was initiated in the cell and a wall temperature of 330 °C was first obtained in this location when burnout occurred. This result implies that further CHF improvements could be achieved if the initiation of dryout at the cell can be suppressed.

References:

[1] S. Mori, K. Okuyama, Enhancement of the c ritical heat flux in saturated pool boiling using h oneycomb porous media, International Journal of Multiphase Flow, 35(10) (2009) 946-951.

[2] S. Mori, L. Shen, K. Okuyama, Effect of cel l size of a honeycomb porous plate attached to a heated surface on CHF in saturated pool boilin g, in: the 14th International Heat Transfer Conf erence, ASME, Washington D.C., USA, 2010.

[3] S. Mori, S. Mt Aznam, K. Okuyama, Enhan cement of the critical heat flux in saturated pool boiling of water by nanoparticle-coating and a honeycomb porous plate, International Journal of Heat and Mass Transfer, 80 (2015) 1-6.

[4] M. Arik, A. Bar-Cohen, Effusivity-based co rrelation of surface property effects in pool boili ng CHF of dielectric liquids, International Journ al of Heat and Mass Transfer, 46(20) (2003) 37 55-3764.

[5] S. Mori, S. Mt Aznam, R. Yanagisawa, K. O kuyama, CHF enhancement by honeycomb por ous plate in saturated pool boiling of nanofluid, Journal of Nuclear Science and Technology, (2 015) 1-8.

[6] H. Nakamura, Temperature Measurement U sing Infrared Thermography and Its Application to Convective Heat Transfer Measurement, Jou rnal of Heat Transfer Society of Japan, 54(228) (2015) 47-54.